Kinetic solvent effects on the reaction between flavonoid naringenin and 2,2-diphenyl-1-picrylhydrazyl radical in different aqueous solutions of ethanol: An experimental and theore...

ARTICLE *in* JOURNAL OF MOLECULAR LIQUIDS · AUGUST 2014

Impact Factor: 2.52 · DOI: 10.1016/j.molliq.2014.04.015

4 AUTHORS, INCLUDING:

Ayub Kanaani
Damghan University
7 PUBLICATIONS **32** CITATIONS
SEE PROFILE

Davood Ajloo
Damghan University
49 PUBLICATIONS **214** CITATIONS
SEE PROFILE

Journal of Molecular Liquids xxx (2014) xxx–xxx

Contents lists available at ScienceDirect

Journal of Molecular Liquids

journal homepage: www.elsevier.com/locate/molliq

Kinetic solvent effects on the reaction between flavonoid naringenin and 2,2-diphenyl-1-picrylhydrazyl radical in different aqueous solutions of ethanol: An experimental and theoretical study

Morteza Jabbari [a,*], Hakimeh Mir [a], Ayoob Kanaani [a], Davood Ajloo [b]

[a] School of Chemistry, Damghan University, 36716-41167 Damghan, Iran
[b] School of Chemistry, College of Science, University of Tehran, Tehran, Iran

ARTICLE INFO

Article history:
Received 4 December 2013
Received in revised form 12 April 2014
Accepted 18 April 2014
Available online xxxx

Keywords:
Kinetic solvent effect
Naringenin
DPPH radical
Ethanol–water mixtures
Reichardt and KAT parameters
DFT calculations

ABSTRACT

Kinetic study of the reaction of flavonoid naringenin with the stable free radical 2,2-diphenyl-1-picrylhydrazyl (DPPH) was performed in different percentage compositions of aqueous ethanol (50–90% v/v) using spectrophotometric method. The reaction, which follows the mixed second-order rate law, was investigated under pseudo first-order conditions with respect to the DPPH radical, at (25.0 ± 0.1) °C and an ionic strength of 0.1 mol dm^{-3}. The rate of reaction was found to decrease with increasing organic solvent content in binary mixture. The reaction mechanism was inferred from the stoichiometry, kinetics, and product identification. Furthermore, the effects of solvent composition on the reaction rate in the mixed solvents were analyzed in terms of Reichardt parameter (E_T^N), and Kamlet, Abboud and Taft (KAT) solvatochromic parameters (α, β, and π^*). To further investigate the solvent effects we theoretically studied the three antioxidant action mechanisms of naringenin using density functional theory (DFT) method. Reaction enthalpies related to these mechanisms were calculated in gas-phase, water, ethanol and 50–90% (by v/v) ethanol–water. It was found that theoretical findings are in good agreement with experimental results.

1. Introduction

Flavonoids are natural polyphenolic phytochemicals that are found ubiquitously in plants and have been described as health-promoting, disease-preventing dietary supplements and cancer-preventive agents [1]. Moreover, they are extremely safe and low toxicated, which makes them excellent chemopreventive agents. More than 4000 types of biologically active flavonoids have been identified, which can be further divided into flavonols, flavones, flavanols, flavanones, anthocyanidins, and isoflavonoid subclasses [2]. The common structure of flavonoids is the flavan nucleus, which consists of 15 carbon atoms arranged in three rings (phenylchromanone structure, C_6–C_3–C_6). Rings A and B are benzene rings and ring C is a heterocyclic pyran or pyrone. The recent explosion of interest in the bioactivity of the flavonoids of higher plants is due, at least in part, to the potential health benefits of these polyphenolic components as major dietary constituents. Many of pharmacological effects of flavonoids are related to their antioxidant activity, which is a biological function, important in keeping the oxidative stress levels below a critical point in the body. This property of flavonoids may be due to their ability to scavenge free radicals and to synergistic effects with other antioxidants [3].

Naringenin (4′,5,7-trihydroxyflavanone) is one of the polyphenolic compounds that is mostly found in grapefruit and in lower concentrations in tomatoes and tomato-based products [4]. This flavonoid has been shown to inhibit in vitro the growth of cancer cells in human and can exhibit estrogenic, anticarcinogenic, and antioxidative properties [5]. Naringenin has antioxidant and antitumor activity and may play a role in cancer, heart disease, hypertension, circulation, Alzheimer's disease, etc. [6]. Naringenin has also been shown to reduce hepatitis C virus production by infected hepatocytes (liver cells) in cell culture. This seems to be secondary to naringenin ability to inhibit the secretion of very low density lipoprotein by the cells [7].

As has been frequently reported in the literature, phenolic antioxidants are known to act as free radical scavengers via at least three different mechanisms including hydrogen atom transfer (HAT), single-electron transfer–proton transfer (SET–PT) and sequential proton loss electron transfer (SPLET). These mechanisms may co-exist, and depend on solvent properties and radical characters [8]. Some studies have correlated the free radical scavenging activity to the bond dissociation enthalpy (BDE), the ionization potential (IP), the proton dissociation enthalpy (PDE), the proton affinity (PA) and the electron transfer enthalpy (ETE) values [9]. The low BDE, PA and IP values are beneficial to enhance the direct radical scavenging activity in non-polar or polar solvents. However, extremely low IP will enhance the prooxidant danger through direct transfer of an electron to surrounding oxygen [10].

* Corresponding author.
E-mail address: m_jabari@du.ac.ir (M. Jabbari).

http://dx.doi.org/10.1016/j.molliq.2014.04.015
0167-7322/

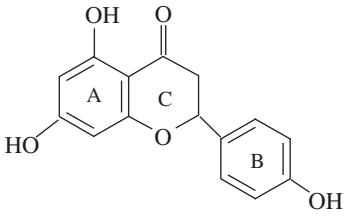

Scheme 1. Chemical structure of naringenin.

In this work, we have performed a detailed kinetic study of the reaction between naringenin and 2,2-diphenyl-1-picrylhydrazyl (DPPH) radical in different aqueous solutions of ethanol (50 to 90% ethanol by v/v) due to the insolubility of naringenin in water. The mechanistic aspects of the reaction are discussed, and the effects of addition of the organic cosolvent to water in the reaction media are also examined, because the information obtained from the results at mixed aqueous solvents can play a crucial role in understanding antioxidant activity. Apart from the experimental studies, a few theoretical investigations mainly based on DFT calculations have also been performed for understanding the relationship between the structure and the antioxidant mechanism of naringenin in the mentioned solvent mixtures. So that, the reaction enthalpies related to the individual steps of three antioxidant action mechanisms (HAT, SET–PT and SPLET) are computed by using DFT/B3LYP method. These calculations are important for providing insight into molecular parameters and also show which mechanism is thermodynamically preferred.

2. Experimental section

2.1. Chemicals

Naringenin (4′,5,7-trihydroxyflavanone), Scheme 1, and 2,2-diphenyl-1-picrylhydrazyl (DPPH) as free stable radical were purchased from Sigma-Aldrich. The solvent ethanol of HPLC gradient grade and tetra-n-butylammonium chloride (TBAC) were obtained from Merck. All chemicals were of reagent grade and were used without further purification. Stock solutions of naringenin and DPPH were freshly prepared by directly dissolving the required amounts of substances in ethanol–water mixture. Dilute solution of these compounds were prepared by adding a known volume of water and organic solvent before recording any kinetic run. The doubly distilled deionized water (conductivity of $1.2 \pm 0.1\ \mu\Omega^{-1}$) was used throughout.

Table 1
The values of k_{obs} at different concentrations of naringenin, constant ionic strength 0.1 mol dm^{-3} (TBAC) and 25 °C.

$10^3 k_{obs}/s^{-1}$					
10^4 [Nar]	Ethanol %				
	50	60	70	80	90
1.80	5.1	5.5	6.2	7.1	7.4
2.16	5.9	6.2	6.9	7.7	7.9
2.52	6.3	6.7	7.5	8.2	8.4
2.88	7.2	7.4	8.3	8.9	9.1
3.24	7.9	8.2	8.7	9.6	9.8

Uncertainties in the pseudo rate constants are 0.1 or lower.

2.2. Kinetics measurements and stoichiometry

The reaction between flavonoid naringenin and the DPPH radical was followed spectrophotometrically by recording the absorbance changes of DPPH at its absorption maximum of 520 nm as a function of time. Earlier it was verified that there is negligible interference from the other reagents at this wavelength. The kinetic measurements were carried out at different percentages for ethanol–water solvents ranging from 50% to 90% (v/v). The progress of the reaction was followed on a UV–vis Cary-50 diode array spectrophotometer (Varian) in conjunction with a Julabo F12 circulating thermobath, using quartz cells of path 10 mm. The temperature was maintained at (25.0 ± 0.1) °C by circulating a thermostated liquid through hollow, thermospacer plates on either side of the cell compartment.

The kinetic runs were performed under pseudo first-order conditions by keeping a large excess of naringenin over the DPPH (1.8×10^{-5} mol dm^{-3}) in all percentages of ethanol–water mixture (with the ratios 18:1, 16:1, 14:1, 12,1, and 10:1 of naringenin to DPPH) and at constant ionic strength (0.1 mol dm^{-3} TBAC). The pseudo first-order rate constants, k_{obs}, for different runs were calculated from the slope of the linear least-square fits of $\ln[1/(A_t - A_\infty)]$ versus time plots, according to the equation: $\ln(1/[A_t - A_\infty]) = k_{obs}t - \ln[A_0 - A_\infty]$, where A_0, A_t and A_∞ are the values of absorbance at zero time, at any time and at the end of the reaction. The A_∞ for each run was taken as the experimentally determined values. The pseudo first-order plots, in all cases, were linear

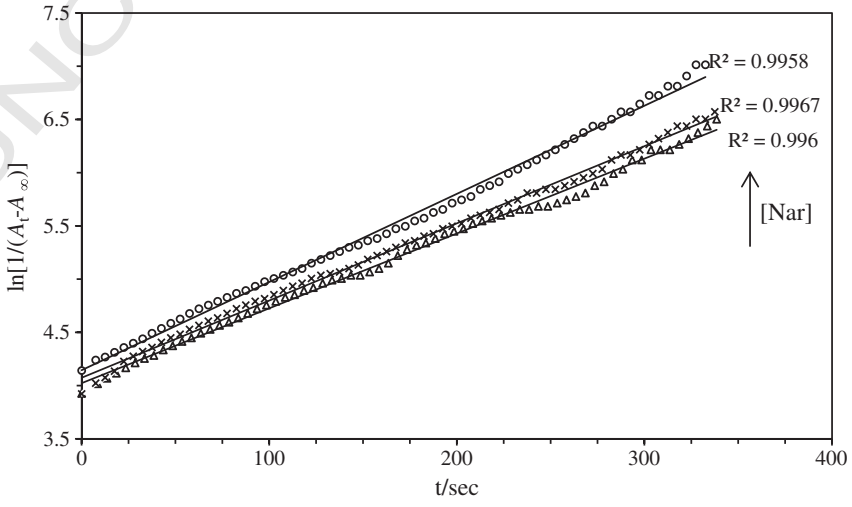

Fig. 1. Plots of $\ln[1/(A_t - A_\infty)]$ versus time in different concentrations of naringenin in 70% ethanol.

Please cite this article as: M. Jabbari, et al., J. Mol. Liq. (2014), http://dx.doi.org/10.1016/j.molliq.2014.04.015

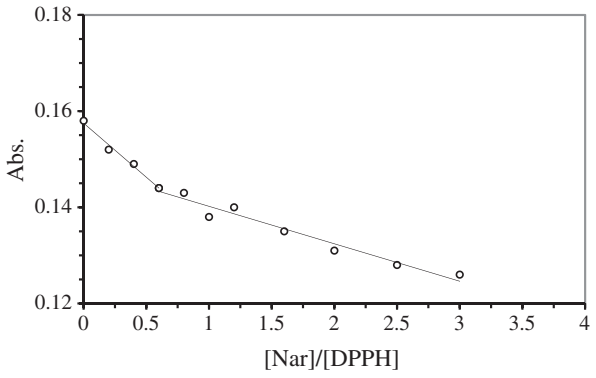

Fig. 2. Molar ratio plot of absorbances of DPPH-naringenin in aqueous solution of ethanol (70% by v/v ethanol) versus mole ratio of reactants at 25 °C and 520 nm.

over 90% completion of the reaction ($r^2 > 0.99$), Fig. 1. The pseudo first-order rate constants (average of at least three distinct determinations) are given in Table 1. Replicate runs showed that the rate constants were reproducible to within ±4%.

To determine the stoichiometric ratios of flavonoid naringenin and the DPPH radical in the reaction under study, the molar ratio method (Yoe–Jones method) was used [11]. The absorbances of a series solutions of DPPH and naringenin in which the concentration of DPPH is held constant (1.8×10^{-5} mol dm^{-3}) while that of the other is varied, were measured at the wavelength of the maximum absorption of the DPPH radical (520 nm) after completion of the reaction. The observed absorbances were plotted versus the mole ratio of the reactants, which showed a break in the slope of the curve at the mole ratio equal to 0.50, corresponding to the combining ratio 2:1 of DPPH:naringenin, Fig. 2. The results indicated an overall of two-electron stoichiometric oxidation of the reaction. Therefore, stoichiometry of the reaction may be given by Eq. (1).

$$H_2L + 2DPPH \rightarrow L + 2DPPH{-}H \quad (1)$$

Where H_2L and L are naringenin and the corresponding quinone product, respectively.

The flavonoid naringenin in water–ethanol solution exhibits two major absorption bands in the UV–vis region (Fig. 3). The absorptions in the 260–310 and 310–360 nm correspond to the A and B ring portions of naringenin, respectively. The spectra are related to the π → π* charge transfer bands in the flavonoid molecule [12]. In this work, the reaction of naringenin with DPPH was followed by produced characteristic changes in the UV–vis spectrum (range 230–390 nm), which did not occur in mixtures without naringenin or DPPH. In keeping with the spectra shown in Fig. 3, after mixing DPPH and naringenin with concentration 1.8×10^{-4} mol dm^{-3}, the repetitive scans of reaction mixture show that the band at 330 and 290 nm increases, so that the increase of the 290 nm band is at a slower rate. These results suggest that the B ring strongly reacts with DPPH radical in respect of the A ring of naringenin. The presence of two isobectic points at 278 and 300 nm suggests that only one absorbant product is formed during the course of naringenin oxidation by DPPH. Since these changes were not observed in the absence of the DPPH radical, they were considered to be the result of DPPH activity. This result is in accordance with the work of Sadik et al. [13], who found similar shifts in the case of oxidation of the flavonoid quercetin under several oxidizing conditions, one of them being a free radical oxidation. Q2

3. Theoretical calculations

All computations have been carried out with the GAUSSIAN 03 Rev. D 01 program package [14]. Density functional theory (DFT) method has been applied because of its excellent compromise between computational time and description of electronic correlation, quantitative structure–activity relationships (QSARs) studies [15]. However, it has been reported that the drug–friccohesity-interaction (DFI) study is a unique experimental study about QSAR [16]. Initial geometry of naringenin generated from standard geometrical parameters was minimized without any constraint in the potential energy surface at Hartee Fock level, adopting the standard 6-31G (d, p) basis set. This geometry was then reoptimized at B3LYP level, using basis as set 6-311G (d, p). A fully relaxed potential energy scan was carried out against the dihedral angle O_{13}–C_1–C_{14}–C_{20} at B3LYP/6-311G(d,p) level. After getting the minimum energy conformations from the energy scan, a further geometry optimization was performed at the B3LYP/6-311++G(d,p) of theory. Vibrational frequencies of the optimized structures were computed by using the same level of theory and thermodynamic corrections [17] were obtained at 298 K and 1 atm, and added to electronic energies. The optimized molecular structure of naringenin that was obtained from GAUSSVIEW 4.1 program is shown in Fig. 4. For phenoxyl radicals (ArO$^{\bullet}$) after removing H atom from the absolute minimum of parent

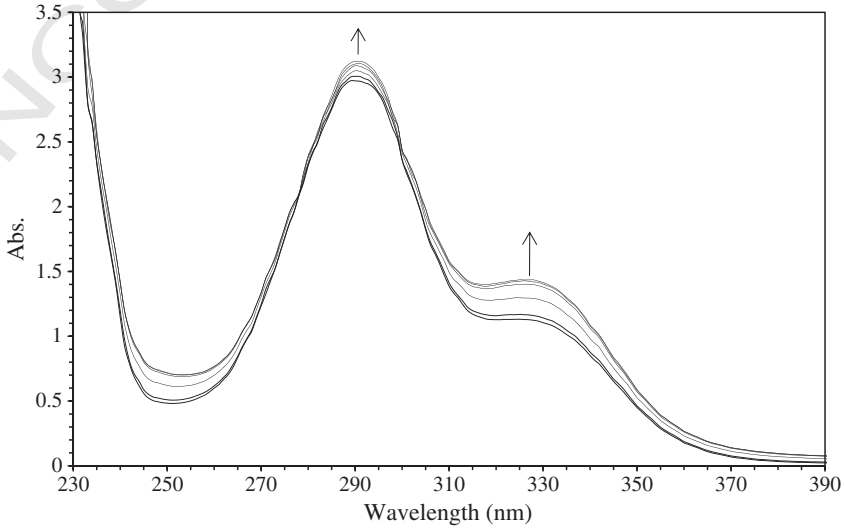

Fig. 3. Consecutive UV–vis spectra obtained in the oxidation of naringenin by DPPH radical at 25 °C and 70% ethanol. Scan speed was at 80 s intervals for 10 min.

Please cite this article as: M. Jabbari, et al., J. Mol. Liq. (2014), http://dx.doi.org/10.1016/j.molliq.2014.04.015

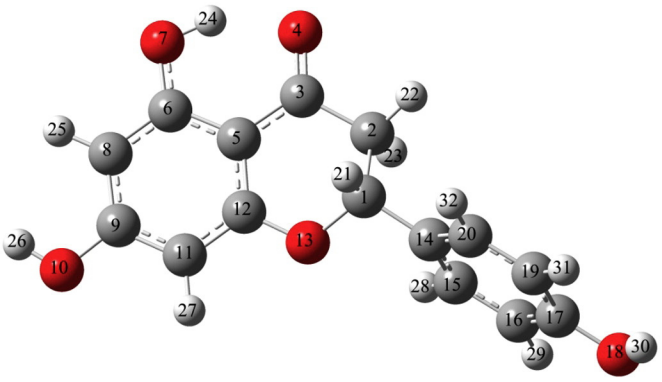

Fig. 4. Optimized geometry of naringenin by B3LYP/6-311++G(d,p).

molecule (ArOH), geometry optimizations and frequency calculations were carried out at the same level of theory and the unrestricted open shell method was applied. No spin contamination was found for radicals, so that the value of $<S^2>$ being 0.75 in all cases.

The molecular quantities such as electronic chemical potential (μ), electronegativity (χ), global hardness (η), global softness (S), electrophilicity indices (ω), polarizability (α) and hyperpolarizability (β) [18] for flavonoid naringenin have computed on the basis of E_{HOMO} and E_{LUMO}, through the following equations

$$\chi = -\frac{1}{2}(E_{LUMO} + E_{HOMO}) \quad (2)$$

$$\mu = \frac{1}{2}(E_{LUMO} + E_{HOMO}) \quad (3)$$

$$\eta = \frac{1}{2}(E_{LUMO} - E_{HOMO}) \quad (4)$$

$$S = \frac{1}{2\eta} \quad (5)$$

$$\omega = \frac{\mu^2}{2\eta} \quad (6)$$

$$\langle\alpha\rangle = \frac{1}{3}\left(\alpha_{xx} + \alpha_{yy} + \alpha_{zz}\right) \quad (7)$$

$$\langle\beta\rangle = \left[\left(\beta_{xxx} + \beta_{yyy} + \beta_{zzz}\right)^2 + \left(\beta_{yyy} + \beta_{yzz} + \beta_{yxx}\right)^2 + \left(\beta_{zzz} + \beta_{zxx} + \beta_{zyy}\right)^2\right]^{\frac{1}{2}} \quad (8)$$

The three mechanisms, which are involved in the radical scavenging properties of phenolic antioxidants (ArOH), HAT, ET–PT and SPLET, are given by Eqs. (9)–(11). All of these may occur in parallel, but with different rates.

$$R^{\cdot} + ArOH \rightarrow ArO^{\cdot} + RH \quad (9)$$

$$1)\quad ArOH + R^{\cdot} \rightarrow ArOH^{\cdot+};\quad 2)\quad ArOH^{\cdot+} + R^{-} \rightarrow ArO^{\cdot} + RH \quad (10)$$

$$1)\quad ArOH \rightarrow ArO^{-} + H^{+};\quad 2)\quad ArO^{-} + R^{\cdot} \rightarrow ArO^{\cdot} + R^{-};\quad 3)\quad R^{-} + H^{+} \rightarrow RH \quad (11)$$

Fig. 5 depicts simplified presentation of HAT, SET–PT and SPLET mechanisms for naringenin as a polyphenolic antioxidant (ArOH).

The reaction given in mechanism HAT (9) is governed by the bond dissociation enthalpy (BDE) of ArOH and RH. To a first approximation, if the BDE of the former is less than that of the latter, the reaction is permitted. The first step in mechanism ET–PT (10) is an electron transfer reaction, whose corresponding controlling parameters are the ionization potential (IP) of ArOH and R^-. A prerequisite for this reaction would be that the IP of the former is lower than that of R^-. The O – H heterolytic bond dissociation enthalpy [proton dissociation enthalpy (PDE)] is involved in mechanism SPLET (11), where the IP of ArO^- is another controlling parameter. To elucidate the third mechanism, proton affinity (PA) and electron transfer enthalpy (ETE) are also taken into consideration.

Total enthalpies of the studied species X, H(X), at the temperature T are usually estimated from the expression (12) [19].

$$H(X) = E_o + ZPE + \Delta H_{trans} + \Delta H_{rot} + \Delta H_{vib} + RT \quad (12)$$

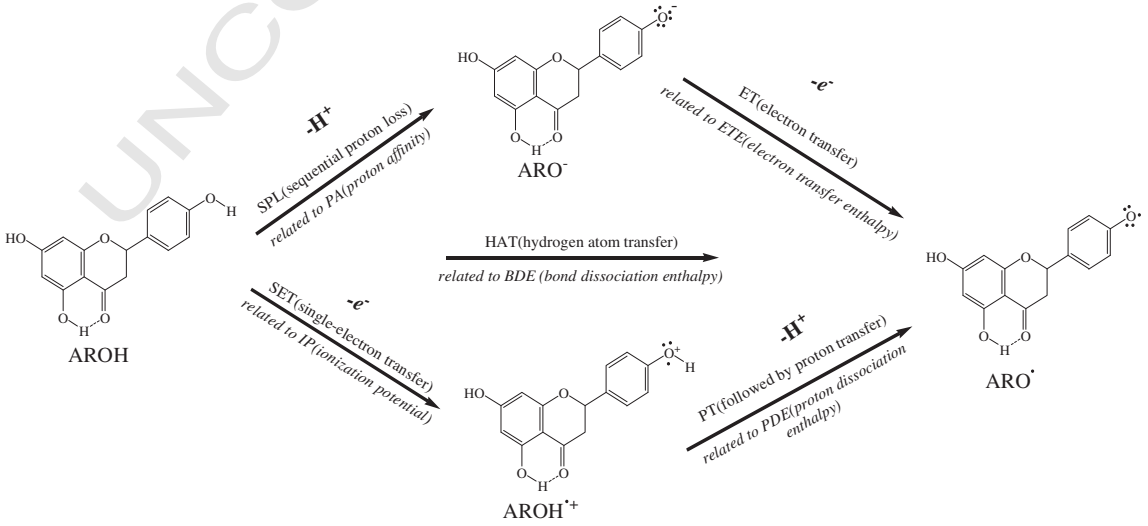

Fig. 5. Simplified presentation of HAT, SET–PT and SPLET mechanisms for naringenin.

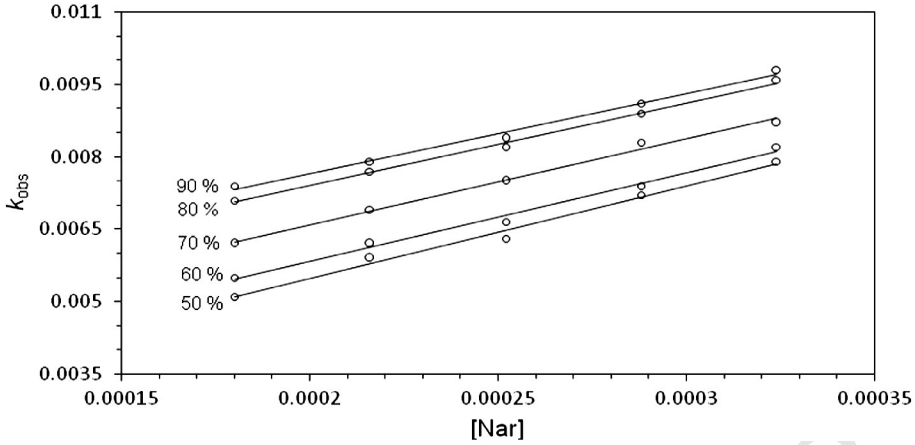

Fig. 6. Plots of k_{obs} versus [nar] in different percentages of aqueous ethanol.

where E_o is the calculated total electronic energy, ZPE stands for zero-point energy, ΔH_{trans}, ΔH_{rot}, and ΔH_{vib} are the translational, rotational, and vibrational contributions to the enthalpy, respectively. Finally, RT represents PV-work term and is added to convert the energy to enthalpy. From calculated total enthalpies we have determined the following quantities

$$BDE = H(ArO^{\cdot}) + H(H^{\cdot}) - H(ArOH) \quad (13)$$

$$IP = H\left(ArOH^{+\cdot}\right) + H(e^{-}) - H(ArOH) \quad (14)$$

$$PDE = H(ArO^{\cdot}) + H\left(H^{+}\right) - H\left(ArOH^{+\cdot}\right) \quad (15)$$

$$PA = H(ArO^{-\cdot}) + H\left(H^{+}\right) - H(ArOH) \quad (16)$$

$$ETE = H(ArO^{\cdot}) + H(e^{-}) - H(ArO^{-\cdot}) \quad (17)$$

4. Results and discussion

The kinetic measurements were performed by using various concentrations of naringenin (1.80×10^{-4} to 3.24×10^{-4} mol dm^{-3}) in 50–90% (by v/v) ethanol–water and 25 °C. It was observed that the k_{obs} values increase with increasing naringenin concentrations in all percentage compositions of aqueous ethanol and decrease by increasing the amount of ethanol in binary mixture, as shown in Table 1.

A nice linear relationship was observed for plots of $\ln[1/(A_t - A_\infty)]$ versus time with DPPH as the limiting reagent, suggesting that the reaction is first order to the DPPH radical. Since it has been proved that the rate-determining step for the oxidation of flavonoids involves the first electron oxidation to form the semiquinone radical intermediate [20], the mechanism of the reaction based on the stoichiometry and the kinetic results therefore can be proposed as:

$$H_2L + DPPH^{\cdot} \xrightarrow{k_2} H_2L^{+\cdot}DPPH^{-} \quad (18)$$

$$H_2L^{+\cdot} + DPPH^{\cdot} \xrightarrow{fast} L + DPPH^{-} + 2H^{+} \quad (19)$$

$$2DPPH^{-} + 2H^{+} \xrightarrow{fast} 2DPPH{-}H \quad (20)$$

Where H_2L is naringenin (nar). According to this mechanism, the rate law can be expressed as

$$rate = k_2[nar][DPPH] \quad (21)$$

Since [nar] ≫ [DPPH], rate = k_{obs}[DPPH] and therefore

$$k_{obs} = k_2[nar] \quad (22)$$

Eq. (22) predicts that the plot of k_{obs} versus [nar] should be a straight line with a positive slope. This equation is consistent with our experimental findings. Similar plots were obtained experimentally (Fig. 6), that support the proposed mechanism. The presence of intercept (non-significant) in these plots is related to the rather low stability of the DPPH radical in ethanol–water solution, which causes a slow natural decay of the DPPH radical in the media. Therefore, the observed rate constant (k_{obs}) for the reaction under study is given by

$$k_{obs} = k_0 + k_2[nar] \quad (23)$$

Table 2
The values of k_2 at various percents of ethanol (v/v), [DPPH] = 1.80×10^{-5} mol dm^{-3}, constant ionic strength 0.1 mol dm^{-3} (TBAC) and 25 °C.

Ethanol %	50	55	60	65	70	75	80	85	90
k_2/ dm^3 mol^{-1} s^{-1}	19.16	18.85	18.33	18.01	17.77	17.39	17.13	16.87	16.69

Uncertainties in the rate constants are 0.05 or lower.

Table 3
The KAT and E_T^N solvatochromic parameters in different ethanol–water mixtures.

Ethanol % v/v	α	β	π^*	E_T^N
50	0.869	0.701	0.970	1.05
55	0.870	0.721	0.933	1.01
60	0.871	0.740	0.895	0.96
65	0.880	0.758	0.856	0.92
70	0.891	0.774	0.816	0.88
75	0.902	0.788	0.776	0.84
80	0.911	0.799	0.736	0.80
85	0.914	0.808	0.698	0.76
90	0.918	0.814	0.660	0.72

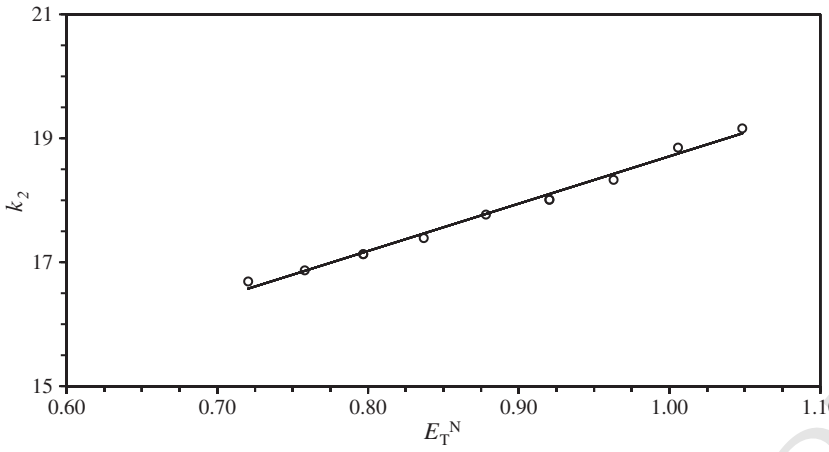

Fig. 7. Plots of k_2 versus E_T^N in different percentages of aqueous ethanol.

where k_0 is the rate constant for the natural decay of DPPH in the medium, and k_2 is the second-order rate constant for the reaction of DPPH with naringenin. These parameters are obtained by plotting k_{obs} against [nar] (Fig. 6) at different composition of binary solvent mixture and are presented in Table 2. As can be seen in Table 2, the second-order rate constants, k_2, increase linearly with decreasing the amount of ethanol in binary mixture.

4.1. Experimental study of solvent effect

In several studies, many efforts have been performed to provide a possible simple description of the solute–solvent interactions treating with the solvent as a continuum possessing a cavity in which the solute molecule is placed [21]. It seems that no single macroscopic physical parameter could possibly account for the multitude of solute–solvent interactions on the molecular microscopic level [22]. A bulk solvent property like dielectric constant can only poorly describe the microenvironment around the reacting species, which govern the stability of the transition state and thus the rate of the reaction.

To obtain a quantitative method for evaluation of the solute–solvent interactions, during the last two decades, many empirical solvent scales have been devised [23]. Among these scales (more than 40), the most comprehensive are the solvatochromic ones, but only a few of them have found a wider application in correlation analysis of solvent effect. A quantitative measurement of the solvent polarity had been introduced by Kamlet, Abboud and Taft (KAT) [24]. The KAT equation contains nonspecific as well as specific solute–solvent interactions separately. In general, these parameters constitute more comprehensive measures of solvent polarity than the dielectric constant alone, because they reflect more reliably the complete picture of all intermolecular forces acting between solute and solvent molecules. This approach has been widely and successfully applied in the correlation analysis of all kinds of solvent-dependent processes [25–27]. Using the solvatochromic parameters α, β, and π^* which have been introduced in previous reports [25–28], the multi-parameters equation [Eq. (24)] has been proposed for use in the so-called Linear Solvation Energy Relationship (LSER).

$$\log\ k = A_0 + s\pi* + a\alpha + b\beta \tag{24}$$

where A_0 represents the regression value of the solute property in reference to solvent cyclohexane, π^* is the index of the solvent dipolarity/polarizability, which is a measure of the ability of a solvent to stabilize a charge or a dipole by its own dielectric effects. The α coefficient represents the solvent hydrogen-bond donor (HBD) acidity, in other words it describes the ability of a solvent to donate a proton in a solvent to a solute hydrogen-bond. The β coefficient is a measure of a solvent hydrogen-bond acceptor (HBA) basicity, and describes the ability of a solvent to accept a proton in a solute to solvent hydrogen-bond. The regression coefficients, a, b, and s measure the relative susceptibilities of the solvent-dependent of log k to the indicated solvent parameters.

In this work, we have also used the polarity scale proposed by Dimoroth and Reichardts, E_T, based on the solvatochromic behavior of pyridinium N-phenoxide betaine dye [23]. This scale has now been revised and normalized to E_T^N, known as the normalized polarity parameter, due to the introduction of SI units. E_T^N is related with the ability of a solvent to stabilize charge separation in the dye. According to this approach, the rate constant values were correlated first with E_T^N as a single linear regression analysis using the computer program Microsoft Excel Linest [29]. The values of KAT and E_T^N parameters for all of the ethanol–water mixtures used in this work were obtained from the plot of each property versus the mole fraction of the organic solvent of the values that were reported in the literature for some other percentages of aqueous solutions of ethanol [30], those are listed in Table 3.

An excellent linear correlation of k_2 versus E_T^N was obtained in the aqueous ethanol mixtures (50–90% v/v), Fig. 7. The second-order rate

Table 4
Regression coefficient of the KAT equation (dual-parameter) of k_2 in different aqueous mixtures of ethanol (50–90% v/v), and [DPPH] = 1.80×10^{-5} mol dm^{-3}.

Regression coefficient [a]	ose [b]	rss [c]	f-test	r^2 [d]
1.38 (0.07) − 0.27 (0.07)β + 0.10 (0.02)π^*	1.21×10^{-3}	8.75×10^{-6}	1208	1.00
0.93 (0.21) + 0.16 (0.20)α + 0.22 (0.04)π^*	2.27×10^{-3}	3.09×10^{-5}	340	0.99
1.75 (0.07) − 0.18 (0.13)α − 0.44 (0.06)β	1.98×10^{-3}	2.35×10^{-5}	447	0.99

(a) Values in the parentheses are the standard error for that coefficient; (b) the overall standard error; (c) the residual sum of squares; (d) regression coefficient.

Please cite this article as: M. Jabbari, et al., J. Mol. Liq. (2014), http://dx.doi.org/10.1016/j.molliq.2014.04.015

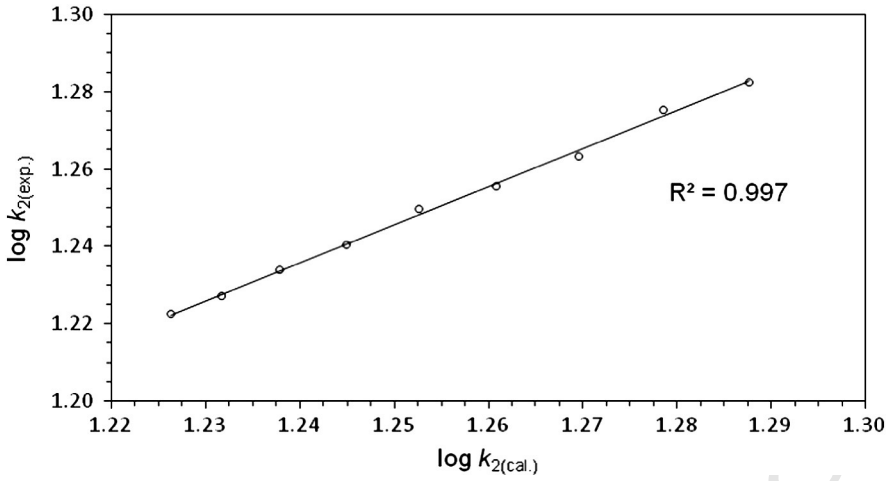

Fig. 8. The experimental second-order rate constants against the rate constants calculated by the dual-parameter of KAT equation with the coefficients *b* and *s* reported in Table 4.

constants of the reaction increase with increasing solvent polarity parameter. This increase is due to a major interaction of polar solvents with the activated complex relative to the reactants; in fact, the polarity of the activated complex of the reaction is higher than those of the reactants. Reactions which are accompanied by an increase in charge separation in their activation process are accelerated in solvents of increasing polarity. The normalized polarity parameter (E_T^N) is a blend of the pure polarity (i.e. dipolarity/polarizability) and hydrogen bonding interactions. In order to show the magnitude of these interactions in the reaction rate, a dual-parameter correlation of log k_2 versus β and π^* and also α and π^* was obtained on the basis of Eq. (24). The obtained results showed that the dual-parameter model using β and π^* parameters represents a significant improvement in the regression analysis with respect to α and π^* as well as α and β dual-parameter models and yield the lowest standard deviation and possess very good coefficients of determination in all cases (Table 4). It can be noticed that the arithmetic signs in front of the coefficients are in agreement with the experimental results. So that, the reaction rate increases with solvent polarity (π^*), whereas its proton-acceptor activity (β), slows it down. Moreover, the negative sign of the coefficients of β parameter suggests that the specific interaction between the reactants and the solvent, via this property, is more than that between the intermediate and the solvent [28].

As can be seen in Table 4, the coefficients of β and π^* are not very different from each other. As a result, β and π^* of the medium have approximately equal effects on the reaction rate. As shown in Fig. 8, the plot of the experimental values of log k_2 versus the calculated one using Eq. (24) with the coefficients of *b* and *s* obtained by the fitting (Table 4), indicates that the interpretations are accurate. However, the single-parameter and multi-parameter correlation of log k_2 versus the KAT solvatochromic parameters (α, β, and π^*) on the basis of Eq. (24) gives poor results together with standard errors of the estimate exceeding the coefficient values.

Owing to the solubility problems of naringenin in water, the second-order rate constant of the reaction cannot be experimentally determined in aqueous medium and so the effect of a very polar solvent like pure water cannot be studied. These observations are similar to other flavonoids reactions [31]. Nevertheless, in the present study, a satisfactory linear relationship between values of k_2 and volume percentages of ethanol was observed in the used mixed solvents, as shown in Fig. 9. The rate constant of naringenin reaction in the pure water, k_{water}, and the pure ethanol, $k_{ethanol}$, can be estimated by the extrapolation of the plot to zero and hundred percent ethanol, respectively. The values of k_{water} and $k_{ethanol}$ obtained from the extrapolation are 22.19 and 16.02 $dm^3\ mol^{-1}\ s^{-1}$, respectively.

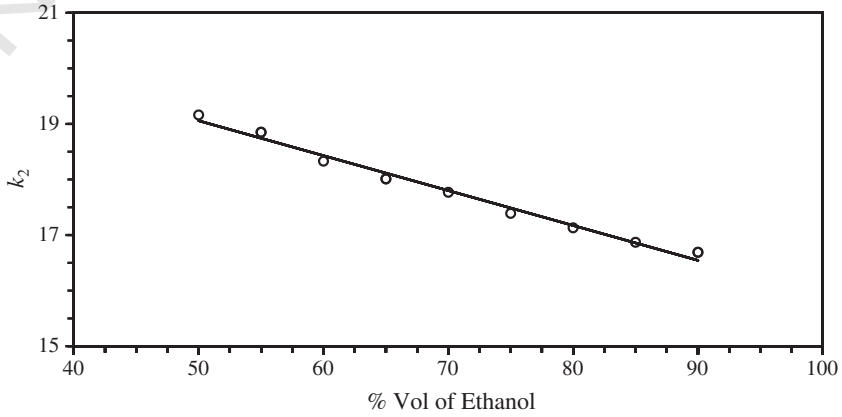

Fig. 9. Plot of k_2 versus % vol of ethanol in different percentages of aqueous ethanol.

Table 5
The values of solvation enthalpies of H$^{\bullet}$, H^+ and e^- in kJ/mol, and dielectric constant (ε) in different aqueous mixtures of ethanol.

Ethanol % (v/v)	$\Delta_{solv}H(H^{\bullet})$	$\Delta_{solv}H(H^+)$	$\Delta_{solv}H(e^-)$	ε[b]
0%	−4[a]	−1090	−153	78.56
50%	5	−1068	−115	52.62
60%	5	−1063	−107	46.71
70%	5	−1059	−99	40.73
80%	5	−1054	−91	34.84
90%	5	−1050	−84	29.19
100%	5	−1045	−76	24.85

[a] Taken from ref. [50].
[b] Taken from ref. [54].

4.2. Solvation enthalpies of electron, proton and hydrogen atom

Solvation enthalpies of electron, proton and hydrogen atom are the enthalpies change of the following reactions, respectively:

$$Solvent_{(solv)} + e^-_{(g)} \rightarrow solvent^-_{(solv)} \quad (25)$$

$$Solvent_{(solv)} + H^+_{(g)} \rightarrow solvent\text{-}H^+_{(solv)} \quad (26)$$

$$Solvent_{(solv)} + H^{\bullet}_{(g)} \rightarrow solvent\text{-}H^{\bullet}_{(solv)} \quad (27)$$

where $solvent_{(solv)}$ represents a molecule of solvent in its cavity, $X_{(solv)}$ means that X is solvated. Solvent may be one of those used in this work, including ethanol, water and aqueous solutions of ethanol (50 to 90% ethanol by v/v).

The calculated gas-phase enthalpy of proton, $H(H^+)$, and electron, $H(e^-)$, is 6.197 and 3.145 kJ mol^{-1}, respectively [32]. For the enthalpy of hydrogen atom (H$^{\bullet}$) hydration we used the reported experimental value $\Delta_{hydr}H(H^{\bullet}) = -4.0$ kJ mol^{-1} [32] and for the solvents where experimental values are not available, the average value $\Delta_{solv}H(H^{\bullet}) = 5$ kJ mol^{-1} was used because in organic solvents $\Delta_{solv}H(H^{\bullet}) \cong \Delta_{solv}H(H_2)$ varies in very narrow (5 ± 1) kJ mol^{-1} range [32]. We utilized −1090 (water) and −1045 kJ mol^{-1} (ethanol) values of $\Delta_{solv}H(H^+)$, and also −153.1(water) and −76 kJ mol^{-1} (ethanol) values of $H_{solv}(e^-)$ from [33]. The solvation parameters of binary EtOH/H_2O mixtures were calculated by using Eq. (28)

$$P_{Mixture} = P_{EtOH}X_{EtOH} + P_{H_2O}X_{H_2O} \quad (28)$$

where P is the property of interest and X is the percentual fraction (v/v) of the components [34]. The values of the $H_{solv}(H^+)$ and $H_{solv}(e^-)$ parameters for aqueous solutions of ethanol (50 to 90% ethanol by v/v) were calculated by the same procedure (see Table 5). The dielectric constant (ε) values for all the water–organic solvent mixtures used in this work have been taken from the literature [35] and are given in Table 5.

The radicalization of the hydroxyl group at the position O_7–H_{24} in naringenin requires the breaking of the hydrogen bond between this group and the C_3═O_4 carbonyl. The major stability differences between these sits and the remaining radicals may be due to the resonance effects that occur in the position of the –CH═CH– group that allows complete delocalization over the whole molecule. This loss of conjugation leads to the formation of a very unstable radical, which has a value of total molecular energy 5.82 kcal/mol higher than that of the radical derived from B ring. The values of total molecular energies are listed in Table 6.

Table 6
The values of O – H_n stretching frequencies (cm^{-1}), BDE_n, IP_n, PDE_n, PA_n and ETE_n, (in kcal/mol) for naringenin as derived from the calculations in vacuum and solvent mediums.

Medium	IP	$\nu(O_{10}–H_{26})$	BDE_{26}	PDE_{26}	PA_{26}	ETE_{26}	Total energy $_{26}$
Gas	205	3806	421	119	180	77	−598,991.93
Ethanol	155	3802	417	86	128	99	−599,002.86
90% v/v	150	3790	415	85	126	97	−599,002.80
80% v/v	144	3776	416	81	115	95	−599,003.31
70% v/v	139	3766	410	79	112	94	−599,003.26
60% v/v	135	3753	410	79	117	92	−599,003.19
50% v/v	129	3730	409	74	114	90	−599,003.14
Water	100	3659	393	66	96	83	−599,003.43

Medium	$\nu(O_{18}–H_{30})$	BDE_{30}	PDE_{30}	PA_{30}	ETE_{30}	Total energy $_{30}$
Gas	3791	388	120	166	72	−598,997.75
Ethanol	3794	392	85	123	93	−598,999.48
90% v/v	3765	395	84	119	93	−598,999.49
80% v/v	3745	397	75	114	92	−598,999.52
70% v/v	3675	398	73	110	91	−598,999.55
60% v/v	3635	399	78	107	90	−598,999.57
50% v/v	3609	399	73	104	90	−598,999.61
Water	3537	393	60	93	87	−598,995.31

4.3. Computational analysis of solvent effects

The dielectric constant (ε) of the medium weakens the strength of the O – H bond, consequently increasing the antioxidant activity of the Phenolic acids (PhAs). Accordingly, the vibrational frequency of the O – H mode (ν_{OH}) decreases with increasing dielectric constant of the solvent (Table 6). The decreasing of ν_{OH} with the increasing of ε could be identified in the observed infrared spectra by a red shift of the OH stretching mode and it may be a good indicator for the ease of proton (or hydrogen atom) transfer. This observation may be explained by the fact that electrostatic interactions between charged particles are all the weaker as the dipole moment of the molecular system increases. One can then argue that, the solvent pushes electrons into the backbone of the molecule, Table 7. These results are consistent with those observed by Clemens et al. [36] on some organic chromophores.

In general, it is a rule of thumb to use free energy as a criterion of the thermodynamically preferred mechanism. However, in the case of the studied reaction, the values of the entropic term $T\Delta S$ do not exceed 4 kJ/mol and all free energies are only shifted in comparison to corresponding enthalpies. Therefore, the thermodynamically preferred mechanism could be derived from comparisons between BDEs, PAs and IPs, since the relative differences between these parameters are largely above the cut-off value of 4 kJ/mol. Moreover, since this work is mainly focused on thermodynamic parameters which do not depend on co-reactive, such species were not considered herein and, are devoted to

Table 7
NPA charges (q/e) on atoms of naringenin as derived from calculations in ethanol, 50% v/v and water.

Atoms	Charges in ethanol	Charges in 50% v/v	Charges in water
H_{21}	0.18	0.18	0.18
H_{22}	0.21	0.21	0.22
H_{23}	0.21	0.21	0.22
H_{24}	0.32	0.34	0.36
H_{25}	0.14	0.15	0.15
H_{26}	0.26	0.27	0.31
H_{27}	0.14	0.15	0.15
H_{28}	0.15	0.16	0.16
H_{29}	0.15	0.16	0.16
H_{30}	0.28	0.30	0.35
H_{31}	0.16	0.16	0.17
H_{32}	0.16	0.16	0.17

Please cite this article as: M. Jabbari, et al., J. Mol. Liq. (2014), http://dx.doi.org/10.1016/j.molliq.2014.04.015

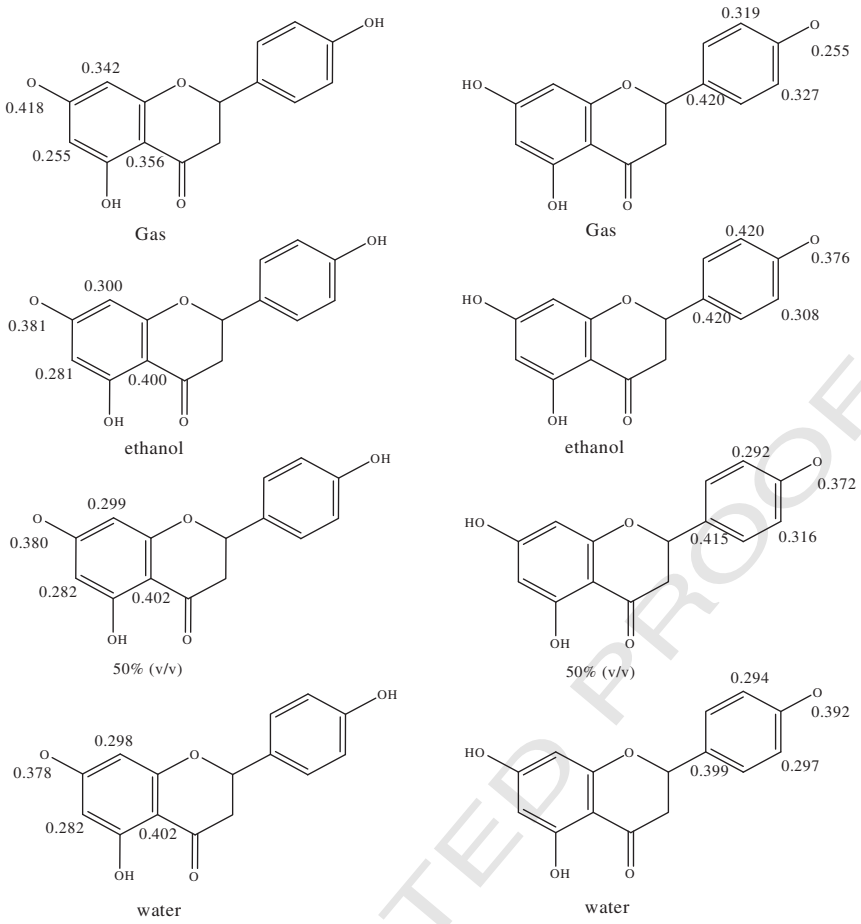

Fig. 10. Distribution of spin densities in the radicals formed by H-removal from the B and A rings for naringenin.

the forthcoming work. In addition, knowing that phenolic hydrogen atoms (or protons) are more acidic than the carboxylic ones [37], we focused all our attention on phenolic hydrogen atoms (or protons).

4.3.1. HAT mechanism

The computed BDE values are reported in Table 6 and are referred to be the most stable species derived from the global minimum for each antioxidant compound. Calculations were performed in gas phase and in solvent since the antioxidants generally work in physiological liquids. The most active system is able to act through the H-atom transfer mechanism both in gas phase and in solution with the smallest BDE. The BDE could serve as a theoretical measure for ranking flavonoids as antioxidants because most active flavonoids possess lower values of BDE. Radical scavenging potency of flavonoids is also mostly related to the presence of OH groups at specific position on the flavonoid core. The minimal value of the BDE of O – H bonds indicates which O – H group of the flavonoid core possesses the most abstract able hydrogen and which O – H group is targeted for radical attack.

Table 8
Dipole moment for neutral molecule and radicals at B3LYP/6-311G(d,p) level of theory.

Solvents	Neutral molecule	O_{18}–H_{30} radical	O_{10}–H_{26} radical
Ethanol	3.6036	3.6614	8.4825
50% v/v	3.5835	3.5403	8.4305
Water	3.6395	3.4000	8.5882

From Table 6 we learn that the homolytic cleavage of H_{30} is easier than that of H_{26} and, $BDE_{30} < BDE_{26}$. In this case, the higher the dielectric constant of the solvent caused the lower the BDE. Going from the vacuum to polar solvents, BDE_{30} and BDE_{26} decrease with the dielectric constant of the solvent, Table 6 for more precise values. So, Solvents with high polarity make easier the homolytic cleavage of H_{30} and H_{26} hydrogen atoms in comparison to the same mechanism happening in the vacuum, the higher the polarity of the solvent, the easier the mechanism. The higher the solvent polarity makes the easier the separation of charges. The important variation on BDE observed with water as solvent, is due to the lower hydration enthalpy of hydrogen, compared to its solvation enthalpy in other solvents, (see Table 5).

4.3.2. SET–PT mechanism

IPs of naringenin obtained in solvent are lower than that obtained in the vacuum, Table 6. The lowest values are associated to polar solvents comparatively to less polar ones. These confirms that polar solvents largely ease the electron transfer. The Polarity values lie in a range of 9.0–5.2 [38]. This result agrees with those pointed out in the literature [37]. Moreover, for naringenin at each solvent, values of IPs are lower than those of BDE_n ($n = 30, 26$) in corresponding solvents, Table 6. Hence, in such solvents, SET–PT is the preferred mechanism than HAT mechanism. This could be due to the high electron solvation enthalpies reported for these solvents, Table 5.

Due to the high solvation enthalpies of proton (Table 5), PDEs of naringenin obtained in solvent is far away lower than that obtained in the vacuum, and the lowest value is observed for ethanol as solvent.

Table 9
Chemical properties of naringenin at B3LYP/6-311G(d,p) level of theory.

Properties	Ethanol	90%	80%	70%	60%	50%	Water
E_{HOMO} (eV)	−6.5401	−6.5405	−6.5409	−6.5412	−6.5401	−6.5420	−6.5439
E_{LUMO} (eV)	−1.9918	−1.9924	−1.9931	−1.9937	−1.9934	−1.9950	−1.9981
Chemical hardness (η)	2.2741	2.2740	2.2739	2.2738	2.2734	2.2735	2.2729
Chemical softness (S)	0.2199	0.2199	0.2199	0.2199	0.2199	0.2199	0.2200
Chemical potential (μ)	−4.2660	−4.2664	−4.2670	−4.2675	−4.2667	−4.2685	−4.2710
Electronegativity (χ)	4.2660	4.2664	4.2670	4.2675	4.2667	4.2685	4.2710
Electrophilicity index (ω)	4.0012	4.0023	4.0035	4.0046	4.0039	4.0070	4.0128

These results are in agreement with the fact that aprotic polar solvents have exceptionally good ability of proton solvation [39].

4.3.3. SPLET mechanism

Solvation enthalpy of proton also affects the proton affinity. This explains the lower PAs obtained in the solvent than that obtained in the vacuum. However, for a given conformer, $PA_n > PDE_n$ (n = 30,26), Table 6. This result is in agreement with the fact that cations easily liberates proton than neutral systems. Moreover, for naringenin, values of PAs related to all phenolic protons in whole medium are lower than BDEs and higher than IPs in corresponding solvents, Table 6. Thus, in such solvents, SPLET is the preferred mechanism. Similar results were obtained theoretically and experimentally on various compounds by others authors [40].

ETEs are higher in solvent than in the vacuum, due to the high solvation enthalpies of the electron in such media, Table 6. Thereby, solvent does not facilitate the electron transfer from anionic system.

4.4. Spin density distribution

The shape of the repartition of the atomic spin densities is presented in Fig. 10. The analysis put forward shows the different reactive sites that could react with radicals and that only weak atomic spin densities can be found on the neighboring cycle from which hydrogen abstraction occurs. Considering naringenin O_{18}–H_{30} radical form in ethanol and water solvent, the spin densities remain localized on the B ring through delocalization on four atoms namely O_{18}(0.376), C_{16}(0.308), C_{19}(0.420), C_{14}(0.420) and O_{18}(0.392), C_{16}(0.297), C_{19}(0.294), C_{14}(0.399) respectively. In naringenin O_{18}–H_{30} radical form, C_{14}, C_{16}, C_{19} are centers of positive spin density and C_{15}, C_{17}, C_{20} are centers of negative spin density whereas O_{10}–H_{26} radical C_9, C_{12} and C_6 are centers of positive spin density. A hydroxyl group increases the stability of a radical, if it is substituted on a carbon with positive spin density and has the opposite effect when it is substituted on a carbon with negative spin density. The more delocalized the spin density in the radical, the easier is the radical formed and thus reduced the BDE. The spin population appears to be slightly more delocalized for radicals issued from the B ring (O_{18}–H_{30}) than for those located on the A ring (O_{10}–H_{26}). For example, the spin density is 0.255 on the oxygen atom in the O_{18}–H_{30} naringenin radical whereas it is 0.418 for the O_{10}–H_{26} radical (in phase gas). As a consequence, the BDE is lower in the B-ring than in the A ring. The spin density for the most stable O_{18}–H_{30} radical of the compound naringenin indicates that the unpaired electron is delocalized over the entire aromatic ring. Hence this center can be the most reactive site of naringenin in scavenging free radicals.

4.5. Electronic properties

The dipole moment represents a generalized measurement of the charge density in a molecule and it constitutes an index of reactivity, which is considered as very important in defining the biological properties especially when they are related to the interaction with enzyme active sites [41]. In Table 8, the dipole moments for optimized conformations of naringenin and radicals at B3LYP/6-311G(d,p) level of computation are given. These values are rather high, reflecting the numerous polarized hydroxyl and/or carbonyl functions distributed over the structures. Dipole moment values lie in a range of 3.400–8.588 D for naringenin showing again that this compound can accommodate itself to their environment on the basis of dipole–dipole interactions.

As it is well known, a high ionization potential indicates that the system does not lose electrons easily and a molecule or atom with a greater electronic affinity tends to take electrons easily [42]. The electronegativity measures a tendency to attract electrons in a chemical species, while the hardness is a measure of the resistance to charge transfer [43]. As can be seen from Table 9, values of electron affinity increase by decreasing ethanol content in binary solvent mixture. Based on the maximum hardness principle, the naringenin in ethanol solvent is found to be more stable than the other considered molecules. As per the results in Table 9, values for all the variables associated with the chemical potential are low. Hence, it can be reasonably concluded that this flavonoid has a tendency to give electrons instead of capturing them, which is a sign of their antioxidant ability.

The nucleophilicity is a measure of the strength of the nucleophiles or their relative affinities for the nuclei, allowing comparisons between

Table 10
Electric properties of the neutral and radicals derived from naringenin, calculated in vacuum and in solvent mediums.

Medium	Neutral		Radical O_{10}–H_{26}		Radical O_{18}–H_{30}	
	Polarizability (a.u.)	Hyperpolarizability (a.u.)	Polarizability (a.u.)	Hyperpolarizability (a.u.)	Polarizability (a.u.)	Hyperpolarizability (a.u.)
Gas	−112.46	101.79	−121.34	210.47	−121.34	304.39
Ethanol	−111.63	133.34	−124.26	277.26	−124.60	383.92
Ethanol 90%	−111.63	133.46	−124.27	277.53	−124.97	380.84
Ethanol 80%	−111.62	133.60	−124.29	277.84	−125.35	377.29
Ethanol 70%	−111.62	133.75	−124.30	278.16	−125.74	373.59
Ethanol 60%	−111.62	133.90	−124.32	278.49	−126.13	369.83
Ethanol 50%	−111.61	134.05	−124.34	278.82	−126.52	366.12
Water	−111.58	134.96	−124.44	280.81	−128.92	343.38

Please cite this article as: M. Jabbari, et al., J. Mol. Liq. (2014), http://dx.doi.org/10.1016/j.molliq.2014.04.015

molecules or between different functional groups in a molecule [44]. Since the nucleophilicity depends on the polarizability and hyperpolarizability of the molecules or their functional groups, the determination of these variables is important for this type of studies [45]. Both highest nucleophilicity as polarizability and hyperpolarizability favors the exchange H/D, indicating which sites are more reactive [45].

Recent studies report that in the reaction of flavonoids against peroxyl or DPPH˙ radicals in polar media, the H-atom transference can occur by SPLET, HAT and SET–PT mechanisms [40,45]. Considering that through these mechanisms phenoxide anions and radicals are generated as intermediates, they were simulated from the three hydroxyl groups. The intermediates were characterized in terms of some electrical properties (polarizability and hyperpolarizability), as well as their total molecular energy. The values of polarizability and hyperpolarizability given in Table 10 suggest that $O_{18}H_{30}$ is the most reactive site of naringenin, by means of a radical mechanism. Also, $O_{10}H_{26}$ is the next important reactive site of naringenin in scavenging free radicals. So that, increasing water content in mixed solvents increases this activity. In this case, radicals derived from B-ring is significantly more stable than those derived from A-ring, and this is the probable reason by which they represent the most important sites of naringenin in the reaction with free radicals.

5. Conclusion

Nowadays growing attention is focused on the antioxidant properties of polyphenols with complex structures such as flavonoids because their extensive conjugated π-electron systems allow ready donation of electrons or hydrogen atoms from the hydroxyl moieties to free radicals. The results of the spectrophotometric studies on the kinetics of DPPH-naringenin in different aqueous solutions of ethanol reported here support this hypothesis that the reaction rate and consequently the rate constants decrease as the amount of ethanol increases in the reaction mixtures, and consequently the antioxidant activity of naringenin decreases. Furthermore, an excellent linear correlation of reaction rate constant values of naringenin reaction with DPPH radical versus E_T^N and also the KAT parameters (β and π^*) was obtained in the different aqueous ethanol mixtures. This means that the polarity of the medium and hydrogen bonding interactions are effective factors on the reaction rate and antioxidant property. From theoretical calculations, it was found that the O_{18}–H_{30} group in naringenin structure is the most favored site for homolytic and heterolytic O – H breaking, in all solvents. This theoretical approach confirms the important role of B ring in the antioxidant properties. Inspection of deprotonation processes of O_{18}–H_{30} and O_7–H_{24} hydroxyl groups has shown that, π electron delocalization plays a major role in the stabilization of products and thus in the lowering of the associated energies. Based on the obtained results, the HAT mechanism is dominant in the gas-phase, whereas the SPLET mechanism represents thermodynamically preferred reaction pathway in water, where PAs of OH groups are considerably lower than corresponding BDEs. The variables related to the chemical potential (electronic affinity, potential of ionization, hardness, softness, electronegativity and electrophilicity) allow to classify naringenin as a flavonoid that has the tendency to give electrons more than to attract them, which demonstrates its antioxidant activity.

References

[1] E. Middleton Jr., C. Kandaswami, T.C. Theoharides, Pharmacol. Rev. 52 (2000) 673–751.
[2] A. Kale, S. Gawande, S. Kotwal, Phytother. Res. 22 (2008) 567–577.
[3] L. Mira, M.T. Fernandez, M. Santos, R. Rocha, M.H. Florencio, K.R. Jennings, Free Radic. Res. 6 (2002) 1199–1208.
[4] P. Ryan, M.J. Hynes, J. Coord. Chem. 61 (2008) 3711–3726.
[5] F.A. Van Acker, M.N. Tromp, G.R. Haenen, W.J. Van der Vijgh, A. Bast, FEBS Lett. 473 (2000) 145–148.
[6] S.A. Chimatadar, S.V. Madawale, S.T. Nandibewoor, Transit. Met. Chem. 32 (2007) 634–641.
[7] K.K. Adari, A. Nowduri, V. Parvataneni, Acta Chim. Slov. 55 (2008) 425–429.
[8] I. Nakanishi, T. Kawashima, K. Ohkubo, H. Kanazawa, K. Inami, M. Mochizuki, S. Fukuzumi, N. Ikota, Org. Biomol. Chem. 3 (2005) 626–629.
[9] L. Torres, A. Carreras, A. Jimenez, E. Brillas, X. Torrelles, J. Rius, L. Julia, J. Org. Chem. 72 (2007) 3750–3756.
[10] J.S. Wright, E.R. Johnson, G.A. DiLabio, J. Am. Chem. Soc. 123 (2001) 1173–1183.
[11] V. Butkovi, L. Klasinc, W. Bors, J. Agric. Food Chem. 52 (2004) 2816–2820.
[12] P.C.H. Hollman, I.C.W. Arts, J. Sci. Food Agric. 80 (2000) 1081–1093.
[13] A. Zhou, O.A. Sadik, J. Agric. Food Chem. 56 (2008) 12081-1291. **Q3**
[14] M.J. Frisch, G.W. Trucks, H.B. Schlegel, G.E. Scuseria, M.A. Robb, J.R. Cheeseman, V.G. Zakrzewski, J.A. Montgomery Jr., R.E. Stratmann, J.C. Burant, S. Dapprich, J.M. Millam, A.D. Daniels, K.N. Kudin, M.C. Strain, O. Farkas, J. Tomasi, V. Barone, M. Cossi, R. Cammi, B. Mennucci, C. Pomelli, C. Adamo, S. Clifford, J. Ochterski, G.A. Petersson, P.Y. Ayala, Q. Cui, K. Morokuma, D.K. Malick, A.D. Rabuck, K. Raghavachari, J.B. Foresman, J. Cioslowski, J.V. Ortiz, A.G. Baboul, B.B. Stefanov, G. Liu, A. Liashenko, P. Piskorz, I. Komaromi, R. Gomperts, R.L. Martin, D.J. Fox, T. Keith, M. Al-Laham, C.Y. Peng, A. Nanayakkara, C. Gonzalez, M. Challacombe, P.M.W. Gill, B. Johnson, W. Chen, M.W. Wong, J.L. Andres, C. Gonzalez, M. Head-Gordon, E.S. Reploge, J.A. Pople, Gaussian 03, Revision D.01, Gaussian, Inc., Pittsburgh, 2005.
[15] W. Kohn, Rev. Mod. Phys. 71 (1999) 1253–1266.
[16] R.K. Ameta, M. Singh, J. Mol. Liq. 190 (2014) 200–207.
[17] W.J. Hehre, L. Radom, P.V.R. Schleyer, J.A. Pople, Ab initio Molecular Orbital Theory, Wiley, New York, 1986.
[18] J. Padmanabhan, R. Parthasarathi, V. Subramanian, P.K. Chattaraj, J. Phys. Chem. A 111 (2007) 1358–1361.
[19] A.K. Chandra, T. Uchimaru, Int. J. Mol. Sci. 3 (2002) 407–422.
[20] W.-L. Chen, W.-S. Li, P.-J. Fu, A. Yeh, In. J. Chem. Kinet. 43 (2011) 147–153.
[21] P.P. Schmidt, J. Chem. Soc. Faraday Trans. 2 (74) (1978) 703–720.
[22] Z. Staszak, A. Bartecki, Spectrosc. Lett. 22 (1989) 1193–1201.
[23] C. Reichardt, T. Welton, Solvents and Solvent Effects in Organic Chemistry, 4th ed. VCH, New York, 2011.
[24] R.W. Taft, J.L.M. Abboud, M.J. Kamlet, J. Org. Chem. 49 (1984) 2001–2005.
[25] M. Jabbari, F. Gharib, J. Solut. Chem. 40 (2011) 561–574.
[26] M. Jabbari, F. Gharib, J. Mol. Liq. 168 (2012) 36–41.
[27] M. Jabbari, F. Gharib, Acta Chim. Slov. 57 (2010) 325–331.
[28] D.S. Bhuvaneshwari, K.P. Elango, J. Mol. Liq. 143 (2008) 147–153.
[29] N. Maleki, B. Haghighi, A. Safavi, Microchem. J. 62 (1999) 229–236.
[30] F. Gharib, A. Farajtabar, A. Masteri Farahani, F. Bahmani, J. Chem. Eng. Data 55 (2010) 327–332.
[31] J.P. Cornard, J.C. Merlin, J. Inorg. Biochem. 92 (2002) 19–27.
[32] M.M. Bizarro, B.J.C. Cabral, R.M.B. dos Santos, J.A.M. Simons, Pure Appl. Chem. 71 (1999) 1249–1256.
[33] J. Rimarcik, V. Lukes, E. Klein, M. Ilcin, J. Mol. Struct. THEOCHEM 952 (2010) 25–30.
[34] S.E. Blanco, E.I. Gasull, F.H. Ferretti, Spectrochim. Acta 59A (2003) 2985-1295. **Q4**
[35] G. Akerlof, J. Am. Chem. Soc. 54 (1932) 4125–4139.
[36] O. Clemens, M. Basters, M. Wild, S. Wilbrand, C. Reichert, M. Bauer, M. Springborg, G. Jung, J. Mol. Struct. THEOCHEM 866 (2008) 15–20.
[37] F.H. Yassin, D.S. Marynick, J. Mol. Struct. THEOCHEM 629 (2003) 223–235.
[38] D. Franco, J. Sineiro, M. Rubilar, M. Sanchez, M. Jerez, M. Pinelo, N. Costoya, M.J. Nunez, Electron. J. Environ. Agric. Food Chem. 7 (2008) 3210–3216.
[39] E. Buncel, H. Wilson, Adv. Phys. Org. Chem. 14 (1977) 133–202.
[40] M. Musialik, R. Kuzmicz, T.S. Pawłowski, G. Litwinienko, J. Org. Chem. 74 (2009) 2699–2709.
[41] J.J. Olivero-Verbel, L. Pacheco-Londono, J. Chem. Inf. Comput. Sci. 42 (2002) 1241–1246.
[42] J.B. Foresman, E. Frisch, Exploring Chemistry with Electronic Structure Methods, 2nd ed. Gaussian, Pitttsburgh PA, 2003.
[43] R.G. Parr, W. Yang, Density Functional Theory of Atoms and Molecules, Oxford University Press, New York, 1989. 1423–1430.
[44] P.B. Yukankis, Organic Chemistry, 7th ed. Prentice-Hall, Inc., USA, 2006.
[45] S. Faizi, H. Siddigi, A. Naz, S. Bano, Lubna, Helvetica Chimica Acta 93 (2010) 466–481 **Q5**

Please cite this article as: M. Jabbari, et al., J. Mol. Liq. (2014), http://dx.doi.org/10.1016/j.molliq.2014.04.015